Central nervous system inflammation induces muscle atrophy via activation of the hypothalamic–pituitary–adrenal axis

Theodore P. Braun,[1,2] Xinxia Zhu,[1] Marek Szumowski,[1] Gregory D. Scott,[2,3] Aaron J. Grossberg,[1,2] Peter R. Levasseur,[1] Kathryn Graham,[4] Sheehan Khan,[5] Sambasivarao Damaraju,[6] William F. Colmers,[7] Vickie E. Baracos,[4] and Daniel L. Marks[1]

[1]Papé Family Pediatric Research Institute, [2]MD/PhD Program, and [3]Department of Pulmonary and Critical Care, Oregon Health & Science University, Portland, OR 97239
[4]Department of Oncology, [5]Department of Computer Science, [6]Department of Laboratory Medicine and Pathology, and [7]Department of Pharmacology, University of Alberta, Edmonton, Alberta T6G 2H7, Canada

Skeletal muscle catabolism is a co-morbidity of many chronic diseases and is the result of systemic inflammation. Although direct inflammatory cytokine action on muscle promotes atrophy, nonmuscle sites of action for inflammatory mediators are less well described. We demonstrate that central nervous system (CNS)–delimited interleukin 1β (IL-1β) signaling alone can evoke a catabolic program in muscle, rapidly inducing atrophy. This effect is dependent on hypothalamic–pituitary–adrenal (HPA) axis activation, as CNS IL-1β–induced atrophy is abrogated by adrenalectomy. Furthermore, we identified a glucocorticoid-responsive gene expression pattern conserved in models of acute and chronic inflammatory muscle atrophy. In contrast with studies suggesting that the direct action of inflammatory cytokines on muscle is sufficient to induce catabolism, adrenalectomy also blocks the atrophy program in response to systemic inflammation, demonstrating that glucocorticoids are requisite for this process. Additionally, circulating levels of glucocorticoids equivalent to those produced under inflammatory conditions are sufficient to cause profound muscle wasting. Together, these data suggest that a significant component of inflammation-induced muscle catabolism occurs indirectly via a relay in the CNS.

CORRESPONDENCE
Daniel L. Marks:
marksd@ohsu.edu

Abbreviations used: ADX, adrenalectomized; CNS, central nervous system; CSA, cross-sectional area; EDL, extensor digitorum longus; Gn, gastrocnemius; HPA, hypothalamic–pituitary–adrenal; i.c.v., intracerebroventricular; IGF-1, insulin-like growth factor 1; KLF15, Krüpple-like factor 15; LLC, Lewis lung carcinoma; LOD, limit of detection; MAFbx, muscle atrophy F-box; MC4R, type 4 melanocortin receptor; MTII, melanotan II; mTOR, mammalian target of rapamycin; MuRF1, muscle ring finger protein 1; PF, pair fed; Veh, vehicle; WGn, white Gn.

Loss of muscle mass is a defining feature of cachexia of chronic disease. Patients suffering from cancer, chronic heart disease, chronic obstructive pulmonary disease, sepsis, and many other conditions experience involuntary weight loss and loss of muscle mass, which contributes significantly to mortality (Morley et al., 2006; Tisdale, 2009). A decrease in volitional food intake is often associated with cachexia but is not solely responsible for the loss of muscle mass, as nutritional supplementation fails to substantially reverse changes in body weight (Evans et al., 1985). A common pathological feature of these disparate conditions is an increase in circulating inflammatory cytokines. Systemic administration of cytokines results in muscle catabolism in experimental animals (Acharyya et al., 2004). Furthermore, genetic (Llovera et al., 1998) or pharmacologic blockade (Fujita et al., 1996) of cytokine signaling attenuates experimental cachexia. Numerous studies have demonstrated that inflammatory cytokines can cause atrophic changes in cultured myotubes, and in vivo studies have demonstrated that activation of inflammatory signaling pathways are fundamental to the atrophy process (Strassmann et al., 1992; Zamir et al., 1994; Acharyya et al., 2004; Doyle et al., 2011). However, the catabolic effects of inflammation in vivo have not been shown to depend exclusively on direct cytokine action on skeletal muscle.

Despite the well documented role of the brain in regulating whole body metabolism, the contribution of central nervous system (CNS) inflammation to muscle atrophy has not

The Rockefeller University Press $30.00
J. Exp. Med. Vol. 208 No. 12 2449-2463
www.jem.org/cgi/doi/10.1084/jem.20111020

been examined. The CNS is a known target of cytokine signaling in cachexia, where cytokines act on neural feeding circuits to mediate anorexia (Scarlett et al., 2007; Grossberg et al., 2010). Multiple inflammatory cytokines are induced in the hypothalami of animals treated peripherally with LPS (Ogimoto et al., 2006) or in tumor-bearing animals (Ropelle et al., 2007). When CNS IL-1 receptors are pharmacologically antagonized during systemic inflammation, anorexia and alterations in peripheral protein metabolism are ameliorated (Layé et al., 2000; Lloyd et al., 2003), suggesting that CNS inflammation plays a critical role in integrating the host response to disease.

In this paper, we present evidence that CNS inflammation is sufficient to induce muscle atrophy independent of substantial peripheral inflammation. Activation of the hypothalamic–pituitary–adrenal (HPA) axis is both necessary and sufficient to explain the catabolic action of central inflammation. Consistent with the role of the brain as a central regulator of metabolic homeostasis, this work implicates CNS cytokine signaling in regulating the muscle catabolism in response to systemic inflammation.

RESULTS

CNS inflammation and muscle catabolism are coincident states

CNS inflammation and muscle catabolism are common features in experimental models of cachexia. Mice treated with LPS or implanted with the Lewis lung carcinoma (LLC) robustly increase the expression of inflammatory cytokines in the hypothalamus (Fig. 1, a and c). LPS administration results in generalized inflammation, as indicated by the up-regulation of both IL-1β and TNF. In contrast, tumor growth resulted only in the up-regulation of IL-1β. Furthermore, after systemic LPS administration, IL-1β expression is strongly induced within the hypothalamic arcuate nucleus as shown by in situ hybridization, demonstrating endogenous production within the CNS (Fig. 1 b). Muscle loss in cachexia occurs as a result of a decrease in protein synthesis and a concomitant increase in protein degradation (Baracos et al., 1995) that occurs principally via the ubiquitin proteasome system (Mitch et al., 1994; Baracos et al., 1995; Price et al., 1996). Muscle-specific E3 ubiquitin ligases, muscle atrophy F-box (*MAFbx* or atrogin-1), and muscle ring finger protein 1 (*MuRF1*; Bodine et al., 2001a; Gomes et al., 2001) are induced in catabolic muscle and are regulated by the forkhead box (Foxo) family of transcription factors (Sandri et al., 2004). Increased expression of *MAFbx* and *MuRF1* occurs in all forms of atrophy studied (Lecker et al., 2004). Simultaneous with central inflammation, the atrophy program is activated in skeletal muscle, marked by the up-regulation of *MAFbx*, *MuRF1*, and *Foxo1* (Fig. 1, a and c), which in the case of tumor-bearing animals occurs in the context of muscle mass loss (Fig. 1 d).

Acute and chronic central administration of IL-1β results in muscle atrophy

To determine whether inflammatory signaling in the CNS plays a role in directing muscle catabolism, mice were administered 10 ng IL-1β or vehicle (Veh) by intracerebroventricular (i.c.v.) injection. To control for the anorectic effects of

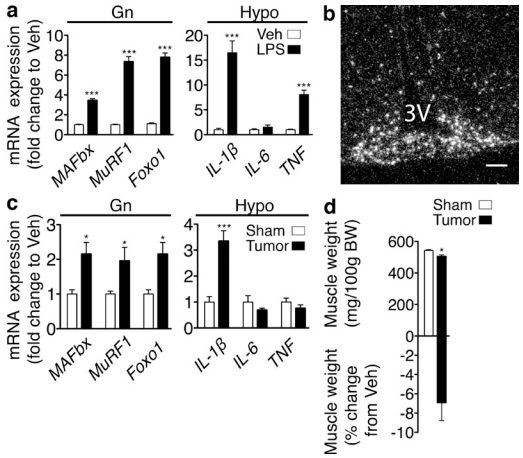

Figure 1. CNS inflammation and muscle catabolism occur simultaneously. (a) Atrophy gene expression in mouse Gn and cytokine expression in mouse hypothalamic blocks (Hypo) 8 h after i.p. LPS (250 µg/kg) or Veh was measured by real-time PCR (n = 5–7/group for Gn and 5/group for Hypo). Values are relative to *GAPDH* for Gn and 18s RNA for Hypo. (b) In situ hybridization for IL-1β mRNA in the arcuate nucleus of the hypothalamus (−2.80 relative to bregma; 3V, third ventricle) 8 h after LPS administration. Veh-treated animals showed no specific signal at this exposure time. (c) Atrophy gene expression in Gn and cytokine expression in hypothalamic blocks in mice bearing LLC tumors (or sham) were measured by real-time PCR (n = 5–9/group). Values are relative to *GAPDH* for Gn and 18s RNA for Hypo. (d) Gn muscle weight normalized to initial body weight (BW) and muscle weight change relative to Veh in LLC tumor bearing animals (n = 5–9/group). Bar, 100 µm. Data are represented as mean ± SEM. *, P < 0.05; ***, P < 0.001 as calculated by unpaired Student's t test.

IL-1β, food was removed from all cages at the time of injection. Central administration of IL-1β led to a significant and rapid induction of *MAFbx*, *MuRF1*, and *Foxo1* mRNA in gastrocnemius (Gn) muscle 4–8 h after the injection (Fig. 2 a), demonstrating rapid activation of the catabolic program in skeletal muscle in response to central inflammation. Given the known role of PI3K/Akt signaling in the regulation of muscle mass, we examined Akt phosphorylation in muscle by Western blot after acute i.c.v. IL-1β (Fig. 2 b). No changes were observed in the phosphorylation of Akt at any time point after i.c.v. IL-1β injection. To rule out the possibility that centrally administered IL-1β was leaking into the systemic circulation and having a direct impact on muscle, we examined p38 MAPK phosphorylation in muscle. Signaling via this pathway occurs downstream of the type I IL-1 receptor (IL-1R1) and has been implicated in the regulation of *MAFbx* (Li et al., 2005; Doyle et al., 2011). No changes were observed in p38 phosphorylation at any time point after central IL-1β injection, suggesting that centrally injected cytokine is unlikely to be directly signaling in muscle (Fig. 2 b). We also examined circulating IL-1β levels after acute central IL-1β injection and found no changes at any time point examined (Table I).

We next examined whether the catabolic molecular mechanisms that are rapidly engaged after bolus i.c.v. IL-1β injection can bring about muscle atrophy with time. Rats were infused with IL-1β into the lateral ventricle for 3 d via

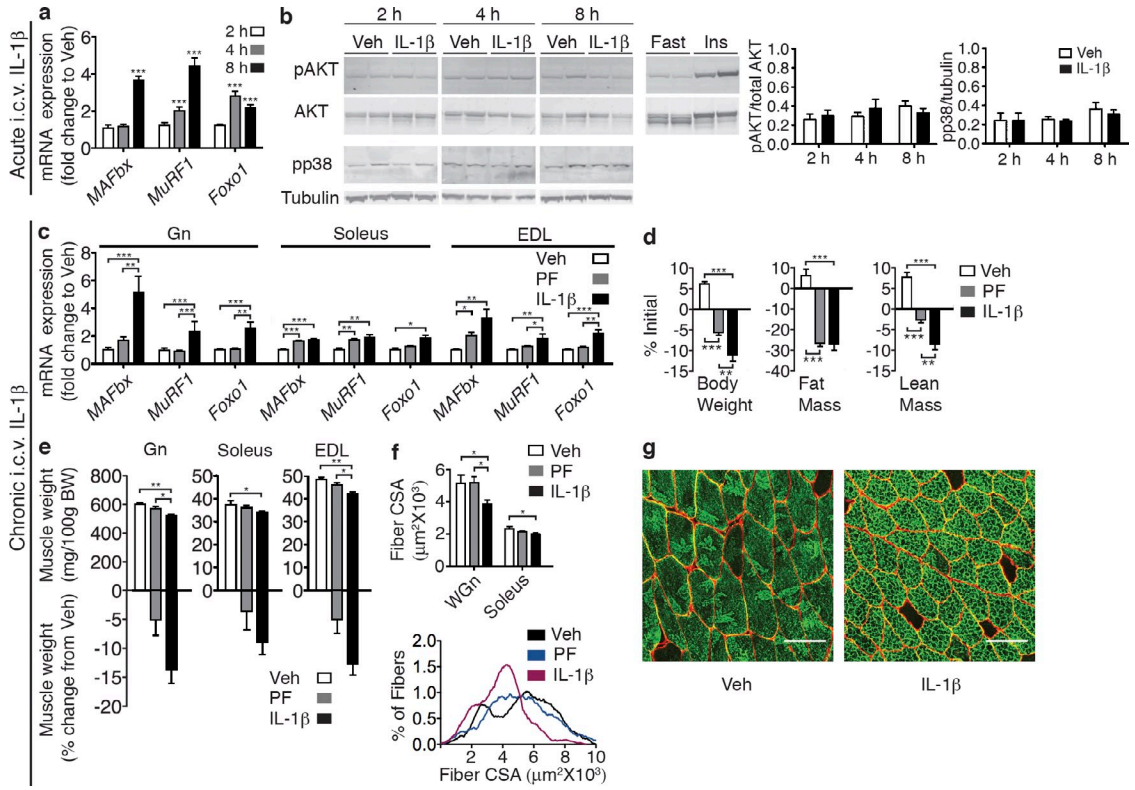

Figure 2. IL-1β signaling in the CNS produces muscle catabolism. (a) Atrophy gene expression in mouse Gn muscle (Gn) after acute i.c.v. IL-1β injection (10 ng, *n* = 6–9/group) or Veh. (b) Akt and p38 phosphorylation in Gn after acute i.c.v. IL-1β was measured by Western blotting (*n* = 6–9/group). (c–g) Rats were i.c.v. infused for 3 d with IL-1β (10 ng/h) or Veh (*n* = 8–11/group). A subset of Veh-treated animals were PF to IL-1β–treated animals. (c) Atrophy gene expression in rat muscle (Gn, Soleus, and EDL) after 3-d i.c.v. IL-1β or Veh infusion was measured by real-time PCR. Reported values are relative to *GAPDH*. (d) Body composition after 3-d IL-1β infusion. (e) Muscle weight normalized to initial body weight (BW) and weight change relative to Veh. (f) Mean fiber CSA in WGn and soleus and frequency distribution in Gn. (g) WGn immunostained for laminin (red), delineating fiber area, and Myosin IIb (green). Bars, 100 µm. Data are represented as mean ± SEM. *, P < 0.05; **, P < 0.01; ***, P < 0.001 calculated by one-way (c–f) or two-way (a and b) ANOVA with Bonferroni's corrected *t* test.

osmotic minipumps at a dose (10 ng/h) thought to mimic endogenous pathophysiologic concentrations under inflammatory conditions (Plata-Salamán et al., 1996). This dose is also far below those given peripherally to induce muscle catabolism or anorexia (Bodine et al., 2001a; Whitaker and Reyes, 2008). To control for the effects of IL-1β on food intake, a subset of Veh-treated animals was pair fed (PF) to the IL-1β–treated animals. Central IL-1β treatment led to a sustained decrease in food intake over the course of the 3-d study. Although Veh-treated animals consumed 78.6 ± 2.2 g of food over the 3-d period, IL-1β–treated animals only consumed 45.29 ± 4.0 g. Similar to acute injection, chronic i.c.v. infusion of IL-1β increased the expression of *MAFbx*, *MuRF1*, and *Foxo1* mRNAs in muscle (Fig. 2 c). The most pronounced differences were seen in the Gn and extensor digitorum longus (EDL), which are predominantly composed

Table I. Circulating cytokines, growth factors, and hormones in acute IL-1β–treated mice

Treatment	IL-6	IL-1β	IGF-1	Corticosterone
	pg/ml	*pg/ml*	*ng/ml*	*ng/ml*
2-h Veh	13 ± 3	22 ± 6	225 ± 11	104 ± 16
2-h 10-ng IL-1β	298 ± 35***	25 ± 6	216 ± 18	397 ± 30***
4-h Veh	21 ± 6	16 ± 3	200 ± 8	103 ± 14
4-h 10-ng IL-1β	69 ± 14	28 ± 6	168 ± 9	258 ± 35***
8-h Veh	13 ± 6	46 ± 15	173 ± 4	115 ± 34
8-h 10-ng IL-1β	8 ± 2	32 ± 5	205 ± 6	72 ± 10

WT mice received i.c.v. injections of IL-1β. Animals were sacrificed at 2, 4, and 8 h after the injection (*n* = 6-9/group). Plasma IL-6, IL-1β, and IGF-1 levels were measured by ELISA and corticosterone was measured by RIA. ***, P < 0.001 versus corresponding Veh-injected control as calculated by two-way ANOVA with Bonferroni's post test.

of fast twitch fibers. These effects were largely independent from food intake as PF animals failed to show similar changes in gene expression. In contrast, the induction of *MAFbx*, *MuRF1*, and *Foxo1* in the soleus was relatively small. Central IL-1β infusion also resulted in significant alterations in body composition, resulting in significant food intake–independent losses of both body weight and lean mass (Fig. 2 d). Although significant fat mass loss occurred with IL-1β treatment, these changes were paralleled by the PF group. Concurrent with the changes in body composition, significant food intake–independent loss of Gn and EDL muscles were observed (Fig. 2 e). To examine whether the loss of muscle mass seen with i.c.v. IL-1β treatment is the result of myofibrillar atrophy, fiber cross-sectional area (CSA) was measured in regions of the Gn and soleus muscle composed of fast (white Gn [WGn]) and slow (soleus) fibers. WGn fiber CSA was significantly reduced by IL-1β treatment but unaltered in PF animals (Fig. 2, f and g). In contrast, soleus fiber CSA was only mildly reduced (Fig. 2 f).

To confirm that centrally infused IL-1β is not diffusing systemically and acting directly on muscle, we infused IL-1β i.p. at the same dose given i.c.v (10 ng/h) for 3 d. This peripheral IL-1β treatment did not induce *MAFbx*, *MuRF1*, or *Foxo1* mRNA in the Gn, soleus, or EDL (Fig. 3 a). Unlike i.c.v. infusion, i.p. IL-1β delivered at this dose did not affect Gn, soleus, and EDL weights (Fig. 3 b). In addition, peripheral IL-1β infusion did not significantly alter body weight, lean mass, or fat mass (Fig. 3 c) and failed to alter fiber CSA in the WGn or soleus (Fig. 3, d and e). To determine whether low dose systemic IL-1β infusion was causing increases in circulating IL-1β levels, we measured IL-1β in the plasma of these animals. Circulating IL-1β levels were below the limit of detection (LOD) in all samples (LOD = 93.6 pg/ml; not depicted). Collectively, these data demonstrate that inflammation in the CNS is sufficient to induce muscle atrophy, predominantly in fast twitch fibers. Furthermore, IL-1β is a far more potent catabolic mediator when administered centrally than when given peripherally.

Central melanocortin signaling is not necessary for IL-1β–induced muscle atrophy

Pharmacologic blockade of the type 4 melanocortin receptor (MC4R) prevents IL-1β–induced anorexia (Whitaker and Reyes, 2008) and attenuates lean mass loss in experimental cachexia (Marks et al., 2001; Wisse et al., 2001; Cheung et al., 2005). Furthermore, the MC4R is critical to the CNS regulation of many other facets of metabolism (Nogueiras et al., 2007; Perez-Tilve et al., 2010). Finally, inflammatory challenges specifically up-regulate IL-1β mRNA in the arcuate nucleus, which contains the proximal neurons of the central melanocortin system. Based on this, we sought to examine whether the acute food intake–independent changes in muscle catabolism initiated by IL-1β are dependent on signaling at the MC4R. WT mice and mice lacking a functional MC4R (MC4RKO) were injected i.c.v. with 10 ng IL-1β and were sacrificed 8 h after injection. Surprisingly, IL-1β led to a similar increase in the mRNA for *MAFbx*, *MuRF1*, and *Foxo1* in the Gn of both WT and MC4RKO mice (Fig. 4 a). To further examine the role of the central melanocortin system in regulating muscle catabolism independent from its effects on food intake, rats were injected i.c.v. with 1 nmol melanotan II (MTII), an agonist at the type 3 and 4 melanocortin receptors, and were sacrificed 6 h after injection. MTII failed to increase the mRNA for *MAFbx*, *MuRF1*, or *Foxo1* in the Gn (Fig. 4 b). To determine the impact of increased signaling via the MC4R in the chronic state, 1 nmol MTII was administered i.c.v. every 12 h for 36 h (four injections), and animals were sacrificed 2 h after the final injection. To control for the decreased food intake associated with MTII treatment, Veh-injected control animals were PF with MTII-treated animals. Chronic MTII failed to increase the mRNA for *MAFbx* or *Foxo1* relative to PF controls but led to a small increase in *MuRF1* mRNA in the Gn (Fig. 4 c). No changes in the expression of *MAFbx*, *MuRF1*, or *Foxo1* were seen in the soleus (Fig. 4 c). Both MTII-treated and PF animals lost weight over the course of the experiment, but there was no difference between groups (Fig. 4 d). MTII treatment

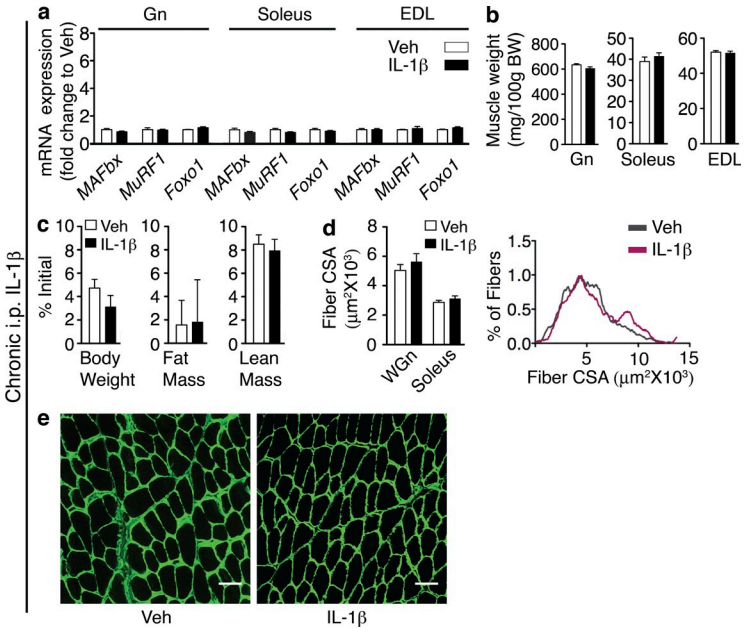

Figure 3. Peripheral infusion of low dose IL-1β does not cause atrophy. Rats were i.p. infused (10 ng/h, n = 7–8/group) for 3 d with IL-1β or Veh solution. (a) Atrophy gene expression in rat muscle (Gn, Soleus, and EDL) after 3-d i.p. IL-1β infusion was measured by real-time PCR. Reported values are relative to *GAPDH*. (b) Muscle weight normalized to initial body weight (BW). (c) Body composition after 3-d IL-1β infusion. (d) Mean fiber CSA in WGn and soleus and frequency distribution in Gn. (e) WGn immunostained for laminin (green) delineating fiber area. Bars, 100 μm. Data are represented as mean ± SEM.

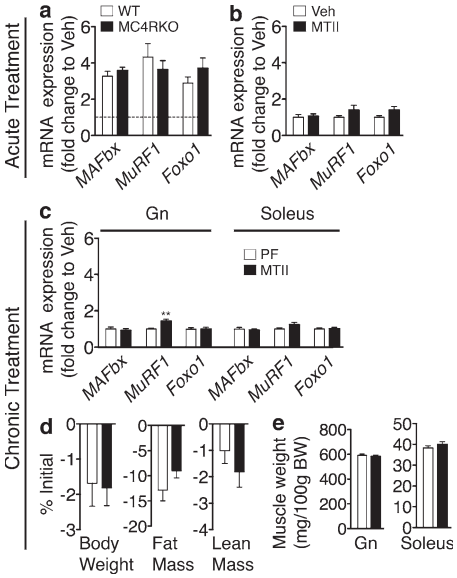

Figure 4. Signaling through the MC4R is not a major contributor to the muscle catabolism independent of food intake. (a and b) Atrophy gene expression in WT and MC4RKO mouse Gn 8 h after acute i.c.v. IL-1β injection (10 ng, $n = 8–9$/group; a) and in rat Gn 6 h after acute i.c.v. MTII (1 nmol, $n = 6–9$/group; b) or Veh injection was measured by real-time PCR. (c–e) Rats were treated for 36 h (chronic) with MTII or Veh (1 nmol/12 h × 4, $n = 7–8$/group). Veh-treated animals were PF to the MTII treatment group. (c) Gene expression in rat Gn and soleus after chronic MTII treatment was measured by real-time PCR. Reported values are relative to *GAPDH*. (d) Body composition after chronic MTII treatment. (e) Muscle weight normalized to initial body weight (BW). The dotted line in a represents Veh-treated controls at a relative quantity of 1. Data are represented as mean ± SEM. **, $P < 0.01$, as calculated by an unpaired Student's *t* test. (a) Analyzed by two-way ANOVA with Bonferroni's corrected *t* test with no significant effect of genotype found. (b, d, and e) Analyzed by unpaired Student's *t* test, with no comparisons reaching $P < 0.05$.

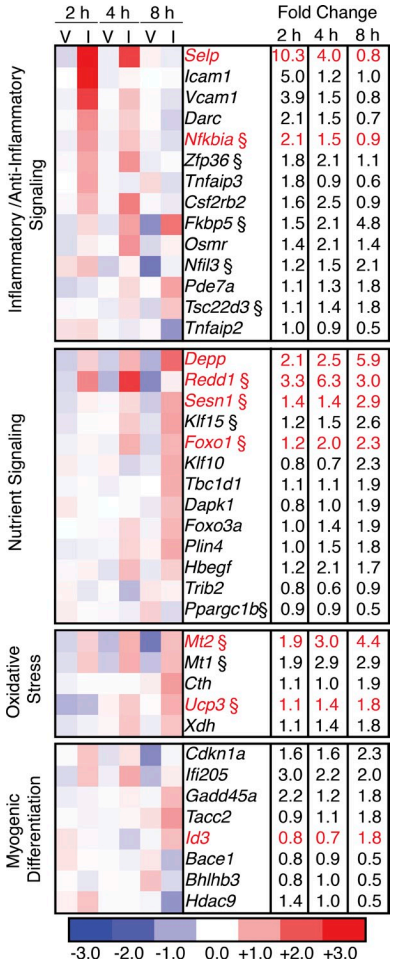

Figure 5. Central IL-1β treatment induces rapid and dynamic changes in skeletal muscle gene expression. WT mice received lateral ventricle injections of IL-1β (I) or Veh (V). Food was removed from the cages at the time of injection, and animals were sacrificed at 2, 4, and 8 h after the injection ($n = 3–5$/group). Skeletal muscle RNA was hybridized to Affymetrix Exon 1.0 ST arrays. Data were analyzed for a false discovery rate of 0.01. Genes that were >1.75-fold up- or down-regulated at any time point were categorized based on their annotated and published functions. Heat map values are $\log_2$ normalized array intensities. Genes with differential expression confirmed by real-time PCR are indicated in red (Fig. S1). § indicates genes that are annotated as glucocorticoid responsive or are regulated in muscle by glucocorticoids in published array datasets.

also did not lead to significant food intake–independent losses of fat mass, lean mass, Gn, or soleus weight (Fig. 4, d and e). These results argue that the CNS mechanism by which IL-1β induces food intake–independent muscle catabolism is not dependent on signaling at the MC4R.

Central IL-1β injection induces a transcriptional program in skeletal muscle, which is analogous to that seen in other forms of atrophy

Changes in the mRNA profile of skeletal muscle undergoing atrophy have been extensively characterized, revealing a conserved pattern of gene expression (Lecker et al., 2004). To gain insight into how central IL-1β induces muscle catabolism, we performed cDNA microarray analysis of mouse skeletal muscle RNA at 2, 4, and 8 h after i.c.v. IL-1β injection. Statistical analysis with a false discovery rate of 1% yielded 494 significantly regulated genes. This list was further narrowed to 100 genes by restricting it to genes that were at least 1.75 fold up- or down-regulated at any of the three time points (Fig. 5, Fig. S1, and Table S2). The expression pattern of 10% of these genes was confirmed by real-time PCR (denoted in red). The complete dataset has been deposited in the GEO Omnibus database (GEO Series accession no. GSE26766). Significantly regulated genes were grouped based on their known functions in skeletal muscle. At the 2- and 4-h time points there was a pronounced regulation of genes involved in regulating the inflammatory/anti-inflammatory balance. At the 4- and 8-h time points, alterations in nutrient signaling were evident, with changes in mammalian target of rapamycin (mTOR) and AMP-activated protein kinase pathway members. An oxidative stress response was also observed at later time points. Genes involved in cell cycle regulation and myogenic differentiation were

Table II. Circulating cytokines, growth factors, and hormones in 3-d IL-1β–treated rats

Treatment	IL-6	IGF-1	Corticosterone
	pg/ml	*ng/ml*	*ng/ml*
Ad lib	106 ± 44	1,075 ± 63	48 ± 29
PF	Undetectable (LOD = 62.5)	851 ± 41*	70 ± 27
IL-1β	102 ± 26	1013 ± 46	183 ± 40*

Rats were infused for 3 d with IL-1β into the lateral ventricle using an osmotic minipump. Control animals were infused over the same time period with a Veh solution and were fed ad lib or PF with IL-1β–treated animals (n = 8–11/group). Plasma IL-6 and IGF-1 were measured by ELISA, and corticosterone was measured by RIA. Data are represented as mean ± SEM. *, $P < 0.05$ versus ad lib control as calculated by one-way ANOVA and Bonferroni's post test or Kruskal-Wallis test and Dunn's multiple comparison post test where appropriate.

significantly affected, suggesting alterations in muscle regeneration. Comparison of this dataset with two separate gene expression array studies evaluating muscle gene expression in response to glucocorticoid administration revealed multiple glucocorticoid-responsive genes (Fig. 5, marked by §; Almon et al., 2007; Wu et al., 2010). These data implicate HPA axis activation in mediating the changes in gene expression in skeletal muscle after central IL-1β treatment.

Regulation of circulating growth factors and cytokines after i.c.v. IL-1β

Plasma levels of IL-6 were examined by ELISA after acute i.c.v. IL-1β injection, as circulating IL-6 increases after central IL-1β administration (De Simoni et al., 1990), and IL-6 has been implicated in mediating muscle catabolism (Fujita et al., 1996). A small induction of circulating IL-6 was observed at early time points, with a peak of 298 ± 35 pg/ml at 2 h versus 13 ± 3 pg/ml in Veh-treated animals, with levels returning to baseline by 8 h (Table I). Despite a marked increase, these levels of IL-6 are quite low in comparison with those found in animals undergoing systemic inflammatory challenge, where peak serum values approach 7,000 pg/ml (Hansen et al., 2000). To examine whether significant IL-6 production or signaling was occurring in muscle after central IL-1β treatment, we measured the expression of IL-6 and its downstream feedback inhibitor suppressor of cytokine signaling 3 (SOCS3). We found no changes in either IL-6 or SOCS3 gene expression in muscle at any time point after central injection of IL-1β, suggesting that significant IL-6 signaling does not occur in muscle after i.c.v. IL-1β injection (unpublished data). Additionally, sustained delivery of IL-1β into the CNS did not lead to an increase in circulating IL-6 levels at the end of 3 d of i.c.v. infusion (Table II), suggesting that the elevation of IL-6 after acute central IL-1β treatment is a transient phenomenon.

Circulating insulin-like growth factor 1 (IGF-1) contributes to the regulation of the anabolic/catabolic balance in skeletal muscle (Stitt et al., 2004). No differences in IGF-1 were observed between Veh and IL-1β–treated animals at any time point, with all values falling in the expected normal range (Table I). IGF-1 levels were also measured in animals infused i.c.v. with IL-1β for 3 d. Serum IGF-1 levels were unaffected by chronic IL-1β administration relative to ad lib–fed controls (Table II).

Glucocorticoids are known mediators of muscle catabolism (Bodine et al., 2001a), and inflammation activates the HPA axis. Given the significant glucocorticoid-regulated gene expression signature seen in response to central inflammation, we measured serum corticosterone (the predominant circulating glucocorticoid in rodents) by radioimmunoassay. Similar to IL-6, serum corticosterone levels were highest at 2 h after acute i.c.v. IL-1β, reaching 397 ± 30 versus 104 ± 16 ng/ml in Veh-treated animals, and had returned to baseline by 8 h after injection (Table I). In contrast with plasma IL-6 levels, chronic i.c.v. infusion of IL-1β led to a sustained increase in circulating corticosterone at the time of sacrifice relative to Veh-treated animals, (183 ± 40 ng/ml for IL-1β–infused animals vs. 37 ± 21 ng/ml for Veh-treated animals; Table II).

Activation of the HPA axis is necessary for the muscle catabolic effects of i.c.v. IL-1β

To explore the involvement of HPA axis activation in i.c.v. IL-1β–induced muscle catabolism, mice received acute i.c.v. injections of 10 ng IL-1β and were treated with the glucocorticoid/progesterone antagonist mifepristone. Mifepristone treatment attenuated the induction of *MAFbx*, *MuRF1*, and *Foxo1* mRNA by i.c.v. IL-1β (Fig. 6 a and Table S1). To confirm these findings, we used adrenalectomized (ADX) mice with low physiological corticosterone replacement. This allowed us to examine whether tonic glucocorticoids are a permissive factor in muscle catabolism or whether an increase in circulating corticosterone is the driver of atrophy. In ADX animals, i.c.v. IL-1β failed to induce *MAFbx* to the same degree as seen in sham-operated animals, and the induction of *MuRF1* and *Foxo1* by i.c.v. IL-1β injection was completely blocked (Fig. 6 b and Table S1). In addition, the induction of the catabolic transcription factor Krüpple-like factor 15 (KLF15), which transactivates *MAFbx* and *MuRF1* (Shimizu et al., 2011), was blocked by ADX. These data demonstrate that an increase in circulating glucocorticoids is necessary for the acute activation of the atrophy program in response to i.c.v. IL-1β.

To determine if intact adrenals are necessary for food intake-independent myofibrillar atrophy, we infused IL-1β or Veh i.c.v. for 3 d in ADX corticosterone-replaced rats. To control for the effects of food intake, Veh-treated animals were PF to IL-1β–treated animals. No significant differences were observed in the expression of *MAFbx*, *MuRF1*, or *Foxo1* in the Gn, soleus, or EDL (Fig. 6 c). There were statistically nonsignificant trends toward an increase in the levels

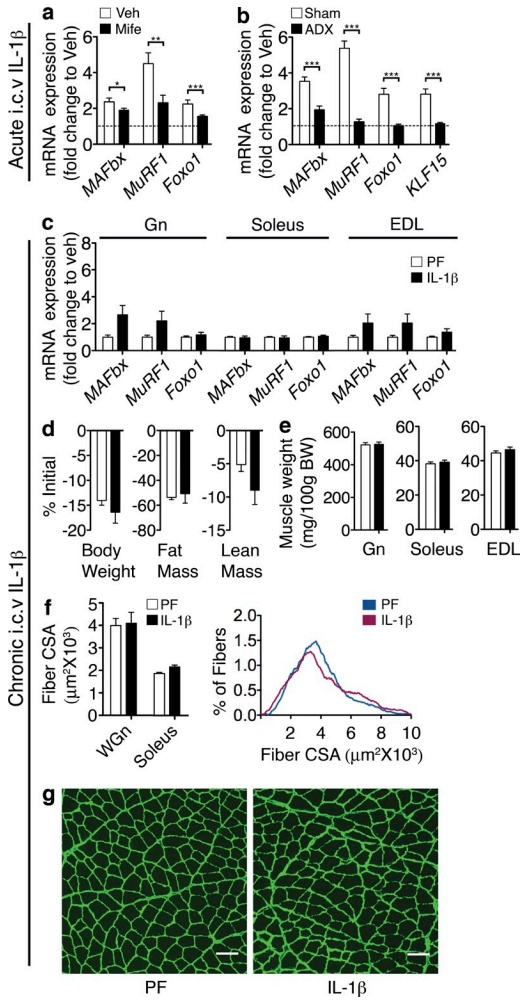

Figure 6. HPA axis activation is necessary for i.c.v. IL-1β–induced muscle catabolism. (a and b) Muscle atrophy gene expression in mifepristone (Mife) or Veh-treated (n = 6–8/group; a) and ADX or sham (n = 7–8/group; b) mouse Gn 8 h after acute i.c.v. 10-ng IL-1β injection was measured by real-time PCR. (c–g) ADX rats were treated for 3 d with chronic i.c.v. IL-1β or Veh (10 ng/h, n = 8–9/group). Veh-treated animals were PF to the IL-1β–treated group. (c) Atrophy gene expression in ADX rat muscle after 3-d chronic i.c.v. IL-1β infusion was measured by real-time PCR. Reported values are relative to *GAPDH*. (d) Body composition. (e) Muscle weight normalized to initial body weight (BW). (f) Mean fiber CSA in WGn and soleus and frequency distribution in WGn. (g) WGn immunostained for laminin (green) delineating fiber area. The dotted lines in a and b represent Veh-treated controls at a relative quantity of 1. Bars, 100 μm. Data are represented as mean ± SEM. *, P < 0.05; **, P < 0.01; ***, P < 0.001 by two-way ANOVA with Bonferroni's corrected t test (a and b; raw data in Table S1) or by unpaired Student's t test (d–g), with no comparisons reaching P < 0.05.

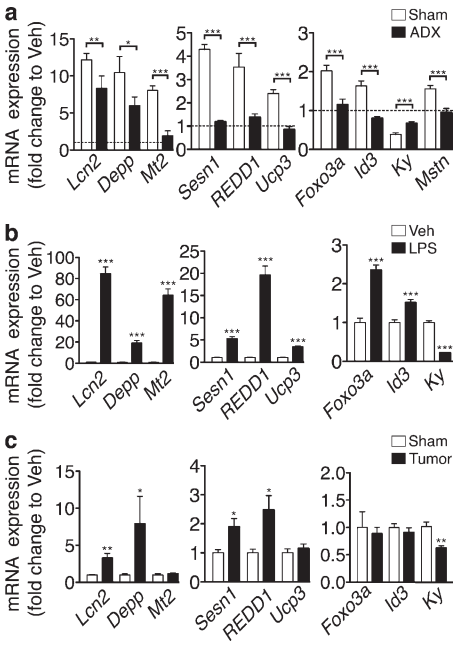

Figure 7. Glucocorticoid-driven gene expression signatures are present in skeletal muscle during central and peripheral inflammation. (a) Gene expression in ADX mouse Gn muscle 8 h after acute i.c.v. 10-ng IL-1β injection or Veh was measured by real-time PCR (n = 6–8/group). (b) Muscle gene expression in mouse Gn 8 h after i.p. LPS (250 μg/kg) or Veh was measured by real-time PCR (n = 5–7/group). (c) Gene expression in Gn in mice bearing LLC tumors (or sham) was measured by real-time PCR (n = 5–9/group). Reported values are relative to *GAPDH*. Data represented as mean ± SEM. The dotted line in a represents Veh-treated controls at a relative quantity of 1. *, P < 0.05; **, P < 0.01; ***, P < 0.001 by unpaired Student's t test (b and c) or two-way ANOVA with Bonferroni's corrected t test (a; raw data in Table S1).

of *MAFbx* and *MuRF1* mRNA in the Gn (*MAFbx* mRNA, P = 0.09; *MuRF1* mRNA, P = 0.12) and EDL (*MAFbx* mRNA, P = 0.19; *MuRF1* mRNA, P = 0.34). Central IL-1β infusion failed to generate a significant decrease in body weight, fat mass, or lean mass beyond that seen in PF animals (Fig. 6 d), although a statistically nonsignificant trend was seen toward the loss of lean mass (P = 0.13). No differences were observed in the weights of Gn, soleus, or EDL muscles (Fig. 6 e). Muscle fiber CSA was also not significantly decreased by IL-1β infusion relative to PF controls in either the WGn or soleus (Fig. 6, f and g). Centrally infused IL-1β was not leaking systemically, as the majority (19/20) of animals had plasma IL-1β levels below the LOD (LOD = 93.6 pg/ml; not depicted).

Central IL-1β induces a glucocorticoid-dependent transcriptional program that is common to models of acute and chronic systemic inflammation

To study the extent to which the transcriptional program initiated by central IL-1β is dependent on glucocorticoid signaling, we selected several genes identified by the array analysis to examine in ADX mice. The adipokine lipocalin-2 (*Lcn2*) and the steroid hormone responsive transcript decidual protein regulated by progesterone (*Depp*) were highly induced by central IL-1β administration, a response only slightly attenuated by adrenalectomy (Fig. 7 a and Table S1). In contrast, the induction of the oxidative stress response genes metallothionein-2 (*Mt2*) and uncoupling protein-3 (*Ucp3*) was completely blocked by ADX. The up-regulation of mTOR

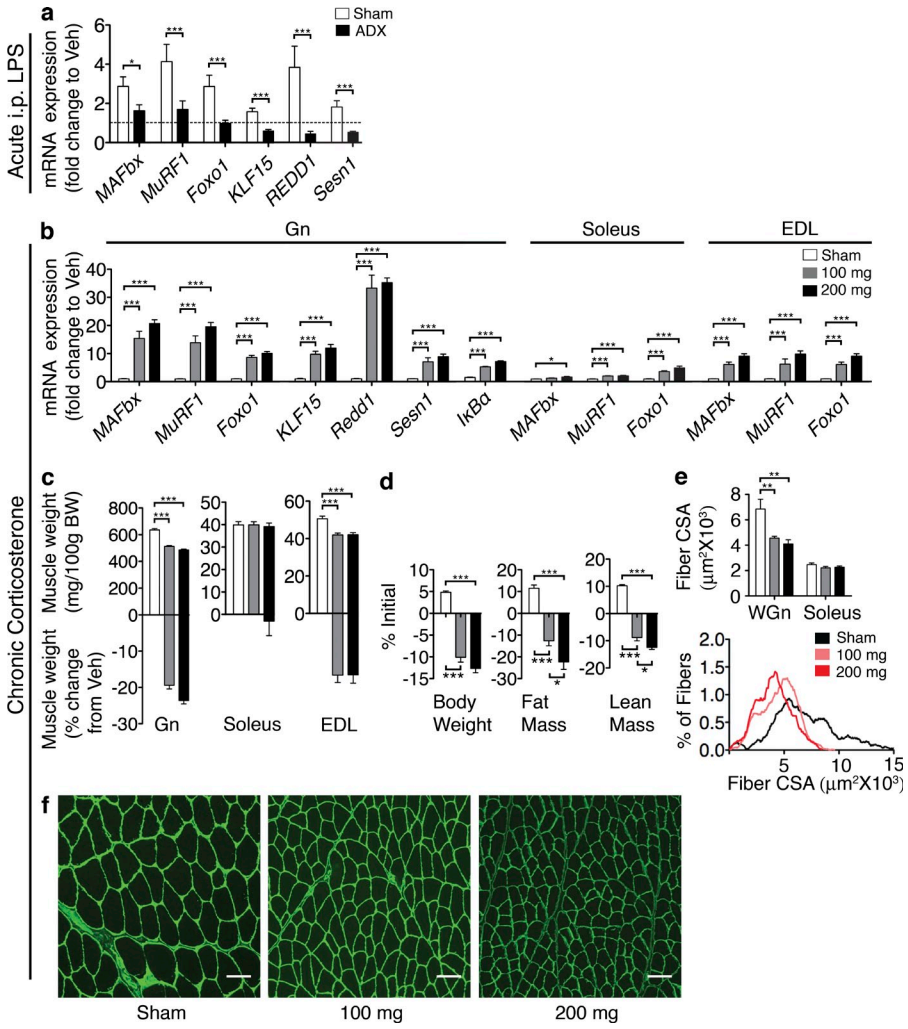

Figure 8. Glucocorticoid signaling contributes to atrophy as a result of systemic inflammation. (a) Gene expression in ADX mouse Gn muscle 8 h after i.p. LPS (250 µg/kg) or Veh was measured by real-time PCR (n = 6–8/group). (b–f) Rats were treated for 3 d with corticosterone (100 or 200 mg; n = 6–7/group). (b) Gene expression in rat muscle (Gn, soleus, and EDL). Reported values are relative to *GAPDH*. (c) Muscle weight normalized to initial body weight (BW) and weight change relative to Veh. (d) Body composition after 3-d corticosterone treatment. (e) Mean fiber CSA in WGn and soleus and frequency distribution in Gn. (f) WGn immunostained for laminin (green) delineating fiber area. The dotted line in a represents Veh-treated controls at a relative quantity of 1. Bars, 100 µm. Data represented as mean ± SEM. *, P < 0.05; **, P < 0.01; ***, P < 0.001 calculated by one-way (b–f) or two-way (a) ANOVA with Bonferroni's corrected t test (raw data in Table S1).

Despite the low-grade peripheral inflammation in tumor-bearing animals, many of the genes examined (five of nine) were regulated in skeletal muscle. Importantly, the glucocorticoid dependent mTOR regulators *Sesn1* and *REDD1* were up-regulated in the muscle of tumor-bearing animals, demonstrating that glucocorticoid signaling may contribute to the pathogenesis of cancer cachexia.

pathway members *Sestrin-1* (*Sesn1*) and regulated in development and DNA damage responses (*REDD1* or *Ddit4*), as well as the downstream target *Foxo3*, was also inhibited by ADX. The anti-myogenic basic helix-loop-helix transcription factor inhibitor of DNA binding 3 (*Id3*) was also induced by central IL-1β treatment in a glucocorticoid-dependent manner. The cytoskeletal protein kyphoscoliosis peptidase (*KY*) is dramatically down-regulated by central inflammation an effect partially blocked by ADX. We also examined myostatin gene expression in skeletal muscle, given its known critical role in the regulation of muscle mass (Zhou et al., 2010; Zhang et al., 2011). Myostatin was modestly induced by central IL-1β administration and this induction was completely blocked by adrenalectomy (Fig. 6 a). Collectively, these genes show a pattern of regulation that is largely dependent on an intact HPA axis, although some features are independently regulated. To confirm this expression pattern in a model of systemic inflammation, we examined the expression of these genes in LPS and tumor-associated muscle catabolism (Fig. 7, b and c). An identical pattern of regulation was observed in LPS-treated animals, suggesting a significant glucocorticoid effect on skeletal muscle in response to peripheral inflammation.

HPA axis activation is necessary and sufficient for muscle wasting driven by central and peripheral inflammation

To examine the role of HPA axis activation in peripheral inflammation-induced activation of the atrophy program, 250 µg/kg LPS was administered to ADX mice. The LPS-mediated induction of *MAFbx* was attenuated in ADX mice, and the induction of *MuRF1* and *Foxo1* were completely prevented in ADX animals (Fig. 8 a). The induction of *KLF15*, *REDD1*, and *Sestrin-1* by LPS was also completely blocked in ADX mice. Collectively, this demonstrates that peripheral inflammation-mediated activation of the atrophy program requires intact adrenal glands.

Although high-dose administration of synthetic glucocorticoids induces substantial atrophy, it remains unknown whether the lower levels of circulating corticosterone evoked by inflammation are sufficient to induce atrophy. To examine this possibility, rats were implanted with sustained release cort pellets at a dose known to produce circulating concentrations approximating levels seen in inflamed animals (Hansen et al., 2000; Kovács et al., 2000). Rats were implanted with 100 or 2 × 100 mg (200 mg) corticosterone tablets, achieving mean circulating levels of 321.8 ± 43.0 and 908.5 ± 223.7 ng/ml,

respectively, versus undetectable levels (LOD = 25 ng/ml) in sham animals. Both treatments significantly induced *MAfbx*, *MuRF1*, and *Foxo1* to largely the same degree (Fig. 8 b). We additionally assessed the expression of the mTOR regulators *REDD1*, *Sestrin-1*, and *KLF15*, as well as the glucocorticoid responsive antiinflammatory mediator *IκBα* (Scheinman et al., 1995), in Gn after corticosterone treatment. All four genes were significantly elevated by 100 and 200 mg corticosterone treatment (Fig. 8 b). Significant weight loss was observed in the Gn and EDL muscle with relative sparing of the soleus (Fig. 8 c). Both 100- and 200-mg treatments also resulted in a significant loss of body weight, fat mass, and lean mass (Fig. 8 d). Significant myofibrillar atrophy was evident in the WGn from both corticosterone treatment groups but was largely absent in the soleus (Fig. 8, e and f). In nearly all cases, little difference was seen between 100- and 200-mg treatments, demonstrating that the atrophy program is maximally activated by corticosterone levels within the physiological range evoked by inflammation.

DISCUSSION

The CNS serves as a central regulator of whole body energy balance coordinating metabolic homeostasis in multiple peripheral tissues (Minokoshi et al., 2002; Nogueiras et al., 2007; Shiuchi et al., 2009). Under normal physiological conditions, anabolism and catabolism are regulated such that energy needs are met. During acute infection, skeletal muscle is mobilized to provide substrates to fuel the necessary increases in immune function. However, in cases of chronic disease where inflammation persists, muscle protein is excessively mobilized, leading to profound muscle atrophy. The regulation of protein mobilization by inflammation occurs at numerous levels. The direct action of inflammatory signaling molecules on skeletal muscle has been extensively examined, as has the contribution of IGF-1 signaling (Bodine et al., 2001b; Rommel et al., 2001; Acharyya et al., 2004; Stitt et al., 2004; Li et al., 2005, 2009; Doyle et al., 2011). The data we present in this paper demonstrate that CNS integration of inflammatory signaling also plays a critical role in regulating the anabolic/catabolic balance in muscle via activation of the HPA axis. Given that a multitude of inflammatory diseases with underlying muscle catabolism are also marked by CNS inflammation, a central mechanism must now be considered when describing muscle atrophy.

To model endogenous production of IL-1β in the CNS and its impact on skeletal muscle, we used i.c.v. injection to deliver physiologically relevant doses of this prototypical inflammatory cytokine. Central injection of IL-1β is believed to mimic its production by the choroid plexus and circumventricular organs (Konsman et al., 2000) and is therefore a model of endogenous inflammation. Hypothalamic IL-1β production is a conserved feature of a multitude of conditions associated with muscle catabolism, including cancer cachexia (Fig. 1; Plata-Salamán et al., 1998; Ropelle et al., 2007), peripheral cytokine administration (Gayle et al., 1997), and endotoxemia (Fig. 1; Ogimoto et al., 2006). Additionally, antagonism of central IL-1 signaling attenuates many of the behavioral (Layé et al., 2000) and metabolic (Gourine et al., 1998; Lloyd et al., 2003) features of inflammatory disease. Our data show that central inflammation initiates significant muscle atrophy. Although we have demonstrated that central Il-1β is sufficient for this effect, it is unlikely to be the only mediator during systemic inflammation, as many cytokines activate the HPA axis (Akita et al., 1995; Bethin et al., 2000). We demonstrate specific production of IL-1β within the arcuate nucleus under inflammatory conditions. The arcuate also contains two neuronal groups that are known to express the IL-1R1: POMC (Scarlett et al., 2007) and AgRP (Scarlett et al., 2008) neurons. The net effect of IL-1β on these two neuronal groups is to increase signaling at the MC4R, decreasing food intake. In accordance with this, the anorexia associated with IL-1β administration is completely prevented by blockade of the MC4R (Whitaker and Reyes, 2008). Furthermore, the loss of lean mass associated with cancer cachexia and LPS administration is prevented by blockade of the MC4R (Marks et al., 2001; Wisse et al., 2001). Surprisingly, we found that signaling at the MC4R is not necessary for central IL-1β–induced muscle catabolism, and MC4R activation is not sufficient to produce significant muscle catabolism. These results are in disagreement with previous work showing a protective effect of melanocortin blockade on body weight and lean mass in experimental cachexia. However, these prior studies did not separate the powerful effects of melanocortin blockade on food intake from its effects on body composition. Given the minor regulation of *MuRF1* by the central melanocortin system, and the effects of the melanocortin system on food intake, it is possible that the protective effects of melanocortin blockade in experimental cachexia are the result of the combination of these two factors alone.

The precise neuroanatomic substrate via which IL-1β exerts its catabolic effect remains unknown. However, given that the major downstream mediator of central inflammation-induced muscle catabolism is activation of the HPA axis, there is significant evidence to implicate endothelial IL-1R1 as a crucial mediator of this effect. Activation of corticotropin-releasing hormone neurons in the paraventricular nucleus (the hypothalamic component of the HPA axis) by central or peripheral IL-1β is blocked by knockdown of endothelial IL-1R1 (Ching et al., 2007). Furthermore, a component of this effect is mediated via endothelium-derived prostaglandin signaling in medullary catecholaminergic neurons projecting to paraventricular neurons, activating the HPA axis (Ericsson et al., 1997; Serrats et al., 2010). Future loss-of-function studies will likely examine the role of inflammatory signaling at the level of the cerebrovascular endothelium in mediating muscle catabolism. In addition, there is a great deal of evidence that pituitary corticotrophs can be directly activated by inflammatory cytokines. Both leukemia inhibitory factor and IL-6 can directly activate pituitary corticotrophs, leading to the release of ACTH independent of hypothalamic signaling (Akita et al., 1995; Bethin et al., 2000).

Increased levels of circulating glucocorticoid are necessary for muscle catabolism as a result of fasting (Wing and Goldberg, 1993), sepsis (Tiao et al., 1996), and acute diabetes (Hu et al., 2009), as adrenalectomy or administration of mifepristone attenuates muscle wasting in these states. Consistent with this, we found that central inflammation also requires an intact HPA axis to induce muscle catabolism. Furthermore, models of peripheral inflammation-induced muscle-wasting share a similar glucocorticoid-responsive gene expression signature, suggesting this response relies on HPA axis activation. Surprisingly, induction of the atrophy program by LPS was almost entirely blocked by adrenalectomy. LPS has been proposed to induce muscle catabolism via direct action on muscle, or via the production of cytokine intermediates such as TNF or IL-1β, which act directly on muscle (Li et al., 2005, 2009; Doyle et al., 2011). Our data suggest that HPA axis activation is an integral part of the catabolic response to inflammation and that glucocorticoids may synergize with cytokines acting directly on muscle to promote atrophy. Interestingly, muscle-specific loss of function of the cytokine receptor adaptor protein TRAF6 ameliorated tumor-induced muscle atrophy, implicating cytokine action on the myocyte as a mediator of atrophy (Paul et al., 2010). However, atrophy as a result of denervation is also attenuated in muscle-specific TRAF6 knockout mice. Given that denervation atrophy is not believed to occur via systemic inflammation, this finding suggests that TRAF6 may play some as yet unspecified role in muscle atrophy independent of its role in transducing inflammatory cytokine signals. Indeed, the inflammatory signaling apparatus has been generally implicated in mediating the atrophic response in skeletal muscle. NF-κB activity is increased in the muscle of tumor-bearing mice, and dominant negative inhibition of NF-κB signaling blocks tumor-associated muscle atrophy (Cai et al., 2004). NF-κB also plays a critical role in the atrophy process in response to denervation and unloading, both of which are not thought to rely on systemic inflammation (Hunter and Kandarian, 2004; Mourkioti et al., 2006). Therefore, it is likely that signaling via TRAF6 and NF-κB plays a fundamental role in atrophy beyond their role in the transduction of systemic inflammatory signals.

Despite the fact that elevated glucocorticoid levels are found in models of cancer cachexia (Rivadeneira et al., 1999), it is widely accepted that they do not participate in muscle atrophy associated with tumor growth (Tessitore et al., 1994; Llovera et al., 1996). However, it is difficult to rule out a role for endogenous glucocorticoids on the basis of these studies. Two of these studies used the same tumor model (YAH-130), which grows in the peritoneal cavity and likely directly impacts organ function. Furthermore, food intake was not removed as a variable in these studies. Despite this, a trend toward improvement was observed in ADX tumor-bearing animals with regard to skeletal muscle protein content (Tessitore et al., 1994). Pharmacologic blockade of glucocorticoid receptors with mifepristone has been unsuccessful in cancer cachexia; however, given the 1–2-h half-life of this drug in rodents (Heikinheimo et al., 1994), the once daily dosing was likely subtherapeutic in these studies. Given the glucocorticoid responsive gene expression signature seen in the skeletal muscle of tumor-bearing animals and the limitations of the aforementioned studies, the involvement of glucocorticoids in tumor-associated muscle wasting appears likely. Future genetic loss-of-function studies will likely shed light on the contribution of glucocorticoids to muscle wasting in cancer.

The molecular mechanisms underlying glucocorticoid-induced atrophy have been extensively studied at the level of skeletal muscle and are driven to a large degree by transcriptional changes. Our array analysis is unique in the literature in that it offers insight into these early transcriptional events that take place after endogenous activation of the HPA axis. The up-regulation of catabolic machinery after central IL-1β administration likely occurs via several molecular mechanisms. Glucocorticoids directly transactivate the *MuRF1* gene in synergy with *Foxo1* (Waddell et al., 2008). In addition, *Foxo1* expression is induced by both central IL-1β and low-dose glucocorticoids. Although the principle mechanism for the regulation of the activity of Foxo transcription factors with regard to their catabolic activity is via Akt-dependent phosphorylation and nuclear exclusion (Sandri et al., 2004), we saw no evidence for alterations in the IGF-1–Akt signaling pathway in response to central inflammation. However, increased levels of *Foxo1* have been extensively correlated with atrophy (Jagoe et al., 2002; Lecker et al., 2004; Sacheck et al., 2007; Shimizu et al., 2011). Furthermore, overexpression of *Foxo1* in muscle is sufficient to produce atrophy (Kamei et al., 2004). Myostatin is another mediator of skeletal muscle catabolism that is induced by central inflammation in an HPA axis–dependent manner. Blockade of myostatin signaling attenuates the induction of *MAFbx* and *MuRF1* in a variety of catabolic states (Zhou et al., 2010; Zhang et al., 2011). *KLF15* is another transcription factor that has recently been implicated in the regulation of skeletal muscle catabolism. *KLF15* is directly induced by glucocorticoids and transactivates both *MAFbx* and *MuRF1* (Shimizu et al., 2011). The suppression of protein synthesis by glucocorticoids is also executed via several distinct mechanisms, all converging to inhibit mTOR signaling. *REDD1* is directly transactivated by the glucocorticoid receptor and inhibits mTOR activity via the tuberous sclerosis complex (Wang et al., 2006). *Sestrin-1* is another negative regulator of mTOR signaling in response to genotoxic stress via activation of the tuberous sclerosis complex and AMPK (Budanov and Karin, 2008). An integral role for sestrin signaling in the catabolic process has not yet been described; however, their role in metabolic signaling cascades makes them likely targets of future studies. Protein synthesis via the mTOR complex is also regulated by the transcription factor KLF15 (Shimizu et al., 2011). The concerted up-regulation of multiple inhibitors of mTOR signaling suggests that central inflammation elicits concerted decreases in protein synthesis and increases in protein breakdown to evoke atrophy.

We found a distinct set of genes that was regulated in skeletal muscle after IL-1β treatment and was not returned to

baseline by adrenalectomy. Although a causative role cannot be ascribed to any of these genes in central IL-1β–induced muscle catabolism, this pattern does demonstrate a glucocorticoid-independent effect of i.c.v. IL-1β on skeletal muscle. Recent work has shown that two discrete events are necessary for muscle catabolism in acute diabetes, where both a loss of skeletal muscle insulin signaling and pathophysiologic levels of glucocorticoid are required (Hu et al., 2009). Critical to the interpretation of these studies is the distinction between physiological levels and pharmacologic dosing of glucocorticoids. It is well known that administration of the synthetic glucocorticoid dexamethasone, in doses far exceeding the physiological range, is sufficient to induce muscle atrophy (Bodine et al., 2001a). However, when dexamethasone is given at a dose estimated to mimic endogenous activation of the HPA axis, no muscle atrophy is observed (Hu et al., 2009). In contrast, we demonstrated that administration of the endogenous glucocorticoid corticosterone, at a dose that mimics the inflammatory activation of the HPA axis, produces dramatic muscle atrophy. This discrepancy is likely a result of the differences between dexamethasone and corticosterone including potency, metabolism, and activity at the mineralocorticoid receptor. Regardless, the levels of circulating corticosterone we achieved in this study are well within the physiological range and comparable with those seen in a multitude of diseases associated with muscle wasting (Tanaka et al., 1990; Llovera et al., 1996). Therefore, it is likely that glucocorticoids are necessary and sufficient to explain a significant portion of muscle catabolism in many forms of chronic disease. However, the incomplete blockade of atrophy gene induction by ADX during both central and systemic inflammation demonstrates that other mechanisms play critical roles in regulating catabolism in response to inflammation.

The finding that CNS inflammation elicits muscle atrophy illustrates a new anatomical target for cytokine-induced muscle catabolism. This study is the first to demonstrate that inflammatory cytokines cause muscle breakdown by acting within the brain. In addition to the direct effects of inflammatory cytokines on skeletal muscle, the action of cytokines in the CNS to influence skeletal muscle metabolism must now be considered. The up-regulation of inflammatory cytokines in the CNS in disease models of cachexia is well documented, indicating that this pathway is generally activated in diseases associated with muscle wasting. Further studies will likely examine the general contribution of the CNS-mediated muscle wasting in cachexia and may discover new therapeutic targets for muscle wasting diseases.

MATERIALS AND METHODS

Animals

20–25-g WT C57BL/6J mice were obtained from The Jackson Laboratory. 250–350-g Sprague Dawley were purchased from Charles River. MC4RKO mice were as used as previously reported (Huszar et al., 1997). MC4RKO mice were backcrossed at least 10 generations into the C57BL/6J strain. All animals were maintained on a normal 12:12-h light/dark cycle and provided ad libitum access to water and food (rodent diet 5001; Purina Mills), except in the case of PF animals in which food intake was restricted to that consumed by the indicated group. Rats were sacrificed by decapitation under isoflurane anesthesia, and mice were sacrificed by decapitation under anesthesia from a ketamine cocktail. Experiments were conducted in accordance with the National Institutes of Health Guide for the Care and Use of Laboratory Animals and approved by the Animal Care and Use Committee of Oregon Health & Science University.

Real-time PCR

Total muscle RNA was extracted using the RNeasy fibrous tissue mini kit (QIAGEN) and hypothalamic RNA was extracted using an RNeasy mini kit according to the manufacturer's instructions. cDNA was transcribed using TaqMan reverse transcription reagents and random hexamers according to the manufacturer's instructions. PCR reactions were run on an ABI 7300 (Applied Biosystems), using TaqMan universal PCR master mix with the following TaqMan gene expression assays: mouse GAPDH (Mm99999915_g1), mouse MAFbx (Mm00499518_m1), mouse MuRF1 (Mm01185221_m1), mouse Foxo1 (Mm00490672_m1), mouse Lcn2 (Mm01324470_m1), mouse Mt2 (Mm00809556_s1), mouse Sesn1 (Mm01185732_m1), mouse DEPP (Mm04206895_m1), mouse UCP3 (Mm00494077_m1), mouse FOXO3 (Mm01185722_m1), mouse Selp (Mm00441295_m1), mouse Nfkbia (Mm00477798_m1), mouse Id3 (Mm00492575_m1), mouse Ky (Mm00600373_m1), mouse REDD1 (Mm00512504_g1), mouse KLF15 (Mm00517792_m1), rat GAPDH (Rn99999916_s1), rat MAFbx (Rn00591730_m1), rat MuRF1 (Rn00590197_m1), rat Foxo1 (Rn01494868_m1), rat IL-1β (Rn00580432_m1), rat KLF15 (Rn00585508_m1), rat REDD1 (Rn01433735_g1), rat Sesn1 (Rn01440906_m1), and rat Nfkbia (Rn01473657_g1; Applied Biosystems). Relative expression was calculated using the ΔΔCt method and was normalized to Veh-treated control. Statistical analysis was performed on the normally distributed ΔCt values. For analyses involving two variables, raw data and two-way ANOVA results can be found in Table S1.

Microarray analysis

Gene expression microarrays were performed in the Department of Oncology at the University of Alberta, Canada.

Synthesis of cRNA and cDNA, labeling, and hybridization of arrays. Protocols and temperature cycling conditions for cDNA synthesis and in vitro transcription of cRNA, hydrolysis of cRNA (by RNase H) and fragmentation (by APE 1), as well as labeling of single-stranded cDNA, were as described by the manufacturers (Ambion and Applied Biosystems) and the WT Expression kit (Ambion). The reaction mix contained 500 ng of total RNA. The reaction mix was spiked with Poly-A RNA (Product Number 900433) to monitor the amplification and labeling process independent of the quality of the initial total RNA used in the reactions. Reaction products at each of the synthesis steps were quantified using the NanoDrop 1000 spectrophotometer. Samples were biotinylated using the WT Terminal Labeling kit (Affymetrix) adhering to the experimental protocols described by the supplier. Samples were hybridized using the Gene Chip Hybridization Control kit (Affymetrix) and the GeneChip Hybridization, Wash, and Stain kit (Affymetrix). Arrays were scanned using the GeneChiP Scanner 3000 7G (Affymetrix).

Gene expression arrays. The total RNA was quantified using a NanoDrop 1000 Spectrophotometer (NanoDrop Technologies) and its integrity evaluated using a Bioanalyzer 2100 (Agilent Technologies) according to the manufacturer's protocols. RNA samples with RNA integrity numbers >5.0 were used in this study (mean of 28 samples is 6.68; maximum value at 8.3 and minimum at 5.1). Mouse expression array (GeneChip Mouse Exon 1.0 ST Array; Affymetrix) were used to capture gene expression profiles in the sample sets. These arrays are designed to capture all exons, each with multiple probes per exon, and are amenable to analysis both for alternatively spliced transcripts (all exons individually) and gene-level expression from multiple probes from exons to yield a single expression level data point reflecting transcripts derived from a single gene. For the current analysis, we used gene-level expression analysis (core analysis) and deferred the exon/splice

variant analysis for future data mining pending development of new analytical tools. The complete dataset has been deposited in the GEO Omnibus database (GEO Series accession no. GSE26766).

Data processing. The gene expression data were normalized and transformed using GeneSpring GX 11.5. Using a Core analysis, the data were summarized using RMA16, log transformed, and baselined to the median in all samples. A one-way ANOVA was performed on the $\log_2$-normalized intensities. After correcting the p-values for multiple comparisons using the Benjamini-Hochberg correction at a false discovery rate of 1%, 494 probes were declared significantly expressed ($P < 2.8 \times 10^{-5}$). Only probes that showed 1.75-fold up- or down-regulation at any of the time points were considered. Genes were organized into functional categories based on GeneRIFs (National Center for Biotechnology Information) and reported function in skeletal muscle (Table S2).

Immunohistochemistry

Cryosections of Gn–soleus complex were cut in cross section. For laminin staining, 20-µm sections were fixed for 15 min in 4% PFA and then blocked in PBS (10 mM $NaPO_4$ and150 mM NaCl)/10% BSA for 1 h at room temperature. Sections were then incubated overnight at room temperature with a rabbit anti-laminin antibody (Sigma-Aldrich) diluted 1:50 in PBS/0.1% BSA, washed with PBS/0.025% Triton X-100, and incubated in a goat anti–rabbit Alexa Fluor 488- or 555-nm labeled secondary antibody (Invitrogen) diluted 1:500 in PBS/10% BSA. Sections were mounted with Vectashield fluorescent mounting media (Vector Laboratories). For analysis of muscle fiber type, 9 µm of unfixed cryosections were blocked for 1 h in PBS/1% BSA/10% goat serum and then incubated overnight in primary antibody diluted 1:250 in PBS/1% BSA/10% goat serum. The following primary antibodies were used: SC-71 for myosin IIa, BF-F3 for myosin IIb (Developmental Studies Hybridoma Bank, University of Iowa, Iowa City, IA), and anti–Myosin I (Vector Laboratories). Sections were washed in PBS/0.025% Triton X-100 and incubated with a goat anti–mouse Alexa Fluor 488 nm–labeled secondary antibody (Invitrogen) diluted 1:500 in PBS/10% BSA. Sections were mounted with Vectashield fluorescent mounting media. Fiber area was measured in images that were acquired on a (DM4000 B microscope; Leica), using a camera (DFC340 FX; Leica) at ambient temperature at 100× magnification using Applications software (Suit 3.6; Leica). Images were segmented in ImageJ (National Institutes of Health) using a coherence enhanced diffusion filter. Images were pseudocolored using ImageJ. Images demonstrating fiber type distribution were obtained using a FW1000 confocal microscope at 100× using FluoView software (Olympus).

LLC tumor implantation

C57BL/6J mice were injected with (1×10^7 cells per site) Tumors were allowed to grow for 21 d and animals were sacrificed. Tumor weight at sacrifice averaged 2.4 ± 0.4 g. Gn muscle and hypothalamic blocks were stored in RNAlater (Ambion) according to the manufacturer's instructions.

i.c.v. injection

For 26-gauge lateral ventricle cannulas (mice) and 22-gauge lateral ventricle cannulas (rats; PlasticsOne) under isoflurane anesthesia, a stereotactic alignment instrument (Kopf) was used at the following coordinates relative to bregma: for mice, −1.0 mm X, −0.5 mm Y, and −2.25 mm Z; for rats, −1.5 mm X, −1.0 mm Y, and −4.0 mm Z. 10-ng mouse IL-1β (R&D Systems) injections were given in 1 µl total volume. IL-1β was dissolved in artificial cerebrospinal fluid (aCSF; 150 mM NaCl, 3 mM KCl, 1.4 mM $CaCl_2$, 0.8 mM $MgCl_2$, and 1.0 mM $NaPO_4$) with 0.1% endotoxin free BSA. MTII (Phoenix Pharmaceuticals) was dissolved in aCSF and administered at 1 nmol/5 µl volume. Chronic injections were performed by administering MTII every 12 h for 36 h (four injections total). 10 mg/kg mifepristone (Sigma-Aldrich) was dissolved in sesame oil and administered 30 min before i.c.v. injection and 4 h after i.c.v. injection.

Chronic lateral ventricle infusions were performed in Sprague Dawley rats using brain infusion kits (Brain Infusion kit II) and osmotic minipumps (model 2001; Alzet). Cannulas were implanted into the lateral ventricle under isoflurane anesthesia, using a stereotactic alignment instrument (Kopf) at the following coordinates relative to bregma: −1.5 mm X, −1.0 mm Y, and −4.0 mm Z. Mini osmotic pumps delivering 10 ng rat IL-1β per hour (R&D Systems) were connected via polyethylene catheters to the cannulas and implanted subcutaneously. Body composition analysis was performed 2 d before surgery, and again immediately before sacrifice, using an EchoMRI 4-in-1 NMR system (EchoMRI).

Peripheral infusions

Mini osmotic pumps (model 1003D; Alzet) delivering 10 ng rat IL-1β per hour were implanted into the peritoneal cavity of Sprague Dawley rats under isoflurane anesthesia. Body composition analysis was performed as per chronic i.c.v. infusion.

LPS treatment

Mice were injected with 250 µg/kg LPS (Sigma-Aldrich) dissolved in normal saline/0.5% BSA and sacrificed 8 h later. For studies examining hypothalamic gene expression, animals were perfused with DEPC-treated PBS before the dissection of hypothalamic blocks to remove circulating immune cells from the tissue.

Adrenalectomy

ADX animals were purchased from Charles River. Animals were implanted with 21-d sustained release corticosterone tablets (Innovative Research of America) immediately after arrival.

Corticosterone pellet implantation

For corticosterone replacement in ADX animal, rats were implanted with 35-mg tablets and mice were implanted subcutaneously with 1.5-mg tablets, both of which are known to produce low physiological levels of corticosterone (Kovács et al., 2000; Pruett and Padgett, 2004). Animals were maintained with 0.9% saline drinking water and allowed to recover at least 1 wk before cannula implantation. To achieve stressed levels of circulating corticosterone, Sprague Dawley rats were implanted with 100- or 2× 100-mg corticosterone tablets which are known to produce circulating levels approximating those seen in stressed animals (Kovács et al., 2000).

Western blotting

Muscles were homogenized in RIPA buffer (50 mM Tris, pH 7.4, 150 mM NaCl, 1 mM EDTA, 1% Triton X-100, 0.25% Na deoxycholate, and 1 mM NaF) and supplemented with Complete protease inhibitors and PhosSTOP phosphatase inhibitor (Roche) for 5 min using a Polytron homogenizer (Kinematica). Samples were incubated on ice for 1 h, and centrifuged at 13,000 RPM for 10 min at 4°C. 50 µg of total protein per lane was run on NuPage Bis-Tris 4–12% gradient polyacrylamide gels (Invitrogen) and transferred to Immobilon-FL PVDF membranes (Millipore). Proteins were detected using the following antibodies and quantitated using an Odyssey System (LI-COR Biosciences): rabbit anti–phospho AKT Ser473 D9E, mouse anti–Pan AKT 40D4, rabbit anti–phospho p38 Thr180/Tyr182 D3F9 (Cell Signaling Technology), E7 tubulin (Developmental Studies Hybridoma Bank), IRDye 800CW goat anti–mouse IgG, and IRDye 680LT goat anti–rabbit IgG (LI-COR Biosciences).

Plasma ELISA and RIA

IL-6 and IGF-1 were measured by ELISA (R&D Systems) according to the manufacturer's instructions. Plasma corticosterone levels were measured by RIA (MP Biomedicals) according to the manufacturer's instructions.

In situ hybridization

Rats were injected with 250 µg/kg LPS and sacrificed 8 h after injection. 20-µm coronal sections were cut on a cryostat and thaw-mounted onto Superfrost Plus slides (VWR Scientific). Hypothalamic sections were collected in a 1:6 series from the diagonal band of Broca (bregma, 0.50 mm) caudally through the mammillary bodies (bregma, 5.00 mm). 0.15 pmol/ml of an antisense ^{33}P-labeled rat IL-1β riboprobe (corresponding to bases 316–762 of rat *IL-1b*; GenBank

accession no. NM_031512.2) was denatured, dissolved in hybridization buffer along with 1.7 mg/ ml tRNA, and applied to slides. Slides were covered with glass coverslips, placed in a humid chamber, and incubated overnight at 55°C. The following day, slides were treated with RNase A and washed under conditions of increasing stringency. Slides were dipped in 100% ethanol, air dried, and then dipped in NTB-2 liquid emulsion (Kodak). Slides were developed 4 d later and cover slipped.

Statistical analysis

Data are expressed as mean ± SEM. Statistical analysis was performed using Prism software (Version 4.0; Prism Software Corp.). All data were analyzed with either an unpaired Student's *t* test, one-way ANOVA followed by a post hoc analysis using a Bonferroni's corrected *t* test, or a two-way ANOVA followed with post hoc analysis using a Bonferroni's corrected *t* test. For the measurements of serum growth factors and hormones, some samples had undetectable levels of the analyte. For these analyses, normal distribution of the data cannot be assumed, and a Kruskal-Wallis test was used with a Dunn's multiple comparison post test. For all analyses, significance was assigned at the level of $P < 0.05$.

Online supplemental material

Fig. S1 shows heat map data for the remainder of the microarray data meeting the inclusion criteria not displayed in Fig. 5. Table S1 contains the raw dCT data from real-time PCR experiments in which two-way ANOVAs were performed and the corresponding p-values. Table S2 contains GenBank accession nos., where available, and p-values for all microarray probe sets meeting the inclusion criteria. Online supplemental material is available at http://www.jem.org/cgi/content/full/jem.20111020/DC1.

Funding was provided by NIH DK 70333, NIH DK 084646, Canadian Institutes of Health Research 200948, and Portland Chapter of Achievement Rewards for College Scientists.

The authors have no relevant commercial affiliations or competing financial interests.

Submitted: 20 May 2011
Accepted: 18 October 2011

REFERENCES

Acharyya, S., K.J. Ladner, L.L. Nelsen, J. Damrauer, P.J. Reiser, S. Swoap, and D.C. Guttridge. 2004. Cancer cachexia is regulated by selective targeting of skeletal muscle gene products. *J. Clin. Invest.* 114:370–378.

Akita, S., J. Webster, S.G. Ren, H. Takino, J. Said, O. Zand, and S. Melmed. 1995. Human and murine pituitary expression of leukemia inhibitory factor. Novel intrapituitary regulation of adrenocorticotropin hormone synthesis and secretion. *J. Clin. Invest.* 95:1288–1298. http://dx.doi.org/10.1172/JCI117779

Almon, R.R., D.C. DuBois, Z. Yao, E.P. Hoffman, S. Ghimbovschi, and W.J. Jusko. 2007. Microarray analysis of the temporal response of skeletal muscle to methylprednisolone: comparative analysis of two dosing regimens. *Physiol. Genomics.* 30:282–299. http://dx.doi.org/10.1152/physiolgenomics.00242.2006

Baracos, V.E., C. DeVivo, D.H. Hoyle, and A.L. Goldberg. 1995. Activation of the ATP-ubiquitin-proteasome pathway in skeletal muscle of cachectic rats bearing a hepatoma. *Am. J. Physiol.* 268:E996–E1006.

Bethin, K.E., S.K. Vogt, and L.J. Muglia. 2000. Interleukin-6 is an essential, corticotropin-releasing hormone-independent stimulator of the adrenal axis during immune system activation. *Proc. Natl. Acad. Sci. USA.* 97:9317–9322. http://dx.doi.org/10.1073/pnas.97.16.9317

Bodine, S.C., E. Latres, S. Baumhueter, V.K. Lai, L. Nunez, B.A. Clarke, W.T. Poueymirou, F.J. Panaro, E. Na, K. Dharmarajan, et al. 2001a. Identification of ubiquitin ligases required for skeletal muscle atrophy. *Science.* 294:1704–1708. http://dx.doi.org/10.1126/science.1065874

Bodine, S.C., T.N. Stitt, M. Gonzalez, W.O. Kline, G.L. Stover, R. Bauerlein, E. Zlotchenko, A. Scrimgeour, J.C. Lawrence, D.J. Glass, and G.D. Yancopoulos. 2001b. Akt/mTOR pathway is a crucial regulator of skeletal muscle hypertrophy and can prevent muscle atrophy in vivo. *Nat. Cell Biol.* 3:1014–1019. http://dx.doi.org/10.1038/ncb1101-1014

Budanov, A.V., and M. Karin. 2008. p53 target genes sestrin1 and sestrin2 connect genotoxic stress and mTOR signaling. *Cell.* 134:451–460. http://dx.doi.org/10.1016/j.cell.2008.06.028

Cai, D., J.D. Frantz, N.E. Tawa Jr., P.A. Melendez, B.-C. Oh, H.G.W. Lidov, P.-O. Hasselgren, W.R. Frontera, J. Lee, D.J. Glass, and S.E. Shoelson. 2004. IKKbeta/NF-kappaB activation causes severe muscle wasting in mice. *Cell.* 119:285–298. http://dx.doi.org/10.1016/j.cell.2004.09.027

Cheung, W., P.X. Yu, B.M. Little, R.D. Cone, D.L. Marks, and R.H. Mak. 2005. Role of leptin and melanocortin signaling in uremia-associated cachexia. *J. Clin. Invest.* 115:1659–1665. http://dx.doi.org/10.1172/JCI22521

Ching, S., H. Zhang, N. Belevych, L. He, W. Lai, X.A. Pu, L.B. Jaeger, Q. Chen, and N. Quan. 2007. Endothelial-specific knockdown of interleukin-1 (IL-1) type 1 receptor differentially alters CNS responses to IL-1 depending on its route of administration. *J. Neurosci.* 27:10476–10486. http://dx.doi.org/10.1523/JNEUROSCI.3357-07.2007

De Simoni, M.G., M. Sironi, A. De Luigi, A. Manfridi, A. Mantovani, and P. Ghezzi. 1990. Intracerebroventricular injection of interleukin 1 induces high circulating levels of interleukin 6. *J. Exp. Med.* 171:1773–1778. http://dx.doi.org/10.1084/jem.171.5.1773

Doyle, A., G. Zhang, E.A. Abdel Fattah, N.T. Eissa, and Y.-P. Li. 2011. Toll-like receptor 4 mediates lipopolysaccharide-induced muscle catabolism via coordinate activation of ubiquitin-proteasome and autophagy-lysosome pathways. *FASEB J.* 25:99–110. http://dx.doi.org/10.1096/fj.10-164152

Ericsson, A., C. Arias, and P.E. Sawchenko. 1997. Evidence for an intramedullary prostaglandin-dependent mechanism in the activation of stress-related neuroendocrine circuitry by intravenous interleukin-1. *J. Neurosci.* 17:7166–7179.

Evans, W.K., R. Makuch, G.H. Clamon, R. Feld, R.S. Weiner, E. Moran, R. Blum, F.A. Shepherd, K.N. Jeejeebhoy, and W.D. DeWys. 1985. Limited impact of total parenteral nutrition on nutritional status during treatment for small cell lung cancer. *Cancer Res.* 45:3347–3353.

Fujita, J., T. Tsujinaka, M. Yano, C. Ebisui, H. Saito, A. Katsume, K. Akamatsu, Y. Ohsugi, H. Shiozaki, and M. Monden. 1996. Anti-interleukin-6 receptor antibody prevents muscle atrophy in colon-26 adenocarcinoma-bearing mice with modulation of lysosomal and ATP-ubiquitin-dependent proteolytic pathways. *Int. J. Cancer.* 68:637–643. http://dx.doi.org/10.1002/(SICI)1097-0215(19961127)68:5<637::AID-IJC14>3.0.CO;2-Z

Gayle, D., S.E. Ilyin, and C.R. Plata-Salamán. 1997. Central nervous system IL-1 beta system and neuropeptide Y mRNAs during IL-1 beta-induced anorexia in rats. *Brain Res. Bull.* 44:311–317. http://dx.doi.org/10.1016/S0361-9230(97)00159-7

Gomes, M.D., S.H. Lecker, R.T. Jagoe, A. Navon, and A.L. Goldberg. 2001. Atrogin-1, a muscle-specific F-box protein highly expressed during muscle atrophy. *Proc. Natl. Acad. Sci. USA.* 98:14440–14445. http://dx.doi.org/10.1073/pnas.251541198

Gourine, A.V., K. Rudolph, J. Tesfaigzi, and M.J. Kluger. 1998. Role of hypothalamic interleukin-1beta in fever induced by cecal ligation and puncture in rats. *Am. J. Physiol.* 275:R754–R761.

Grossberg, A.J., J.M. Scarlett, X. Zhu, D.D. Bowe, A.K. Batra, T.P. Braun, and D.L. Marks. 2010. Arcuate nucleus proopiomelanocortin neurons mediate the acute anorectic actions of leukemia inhibitory factor via gp130. *Endocrinology.* 151:606–616. http://dx.doi.org/10.1210/en.2009-1135

Hansen, M.K., K.T. Nguyen, M. Fleshner, L.E. Goehler, R.P. Gaykema, S.F. Maier, and L.R. Watkins. 2000. Effects of vagotomy on serum endotoxin, cytokines, and corticosterone after intraperitoneal lipopolysaccharide. *Am. J. Physiol. Regul. Integr. Comp. Physiol.* 278:R331–R336.

Heikinheimo, O., U. Pesonen, R. Huupponen, M. Koulu, and P. Lähteenmäki. 1994. Hepatic metabolism and distribution of mifepristone and its metabolites in rats. *Hum. Reprod.* 9:40–46.

Hu, Z., H. Wang, I.H. Lee, J. Du, and W.E. Mitch. 2009. Endogenous glucocorticoids and impaired insulin signaling are both required to stimulate muscle wasting under pathophysiological conditions in mice. *J. Clin. Invest.* 119:3059–3069.

Hunter, R.B., and S.C. Kandarian. 2004. Disruption of either the Nfkb1 or the Bcl3 gene inhibits skeletal muscle atrophy. *J. Clin. Invest.* 114:1504–1511.

Huszar, D., C.A. Lynch, V. Fairchild-Huntress, J.H. Dunmore, Q. Fang, L.R. Berkemeier, W. Gu, R.A. Kesterson, B.A. Boston, R.D. Cone, et al. 1997. Targeted disruption of the melanocortin-4 receptor results in obesity in mice. *Cell*. 88:131–141. http://dx.doi.org/10.1016/S0092-8674(00)81865-6

Jagoe, R.T., S.H. Lecker, M. Gomes, and A.L. Goldberg. 2002. Patterns of gene expression in atrophying skeletal muscles: response to food deprivation. *FASEB J.* 16:1697–1712. http://dx.doi.org/10.1096/fj.02-0312com

Kamei, Y., S. Miura, M. Suzuki, Y. Kai, J. Mizukami, T. Taniguchi, K. Mochida, T. Hata, J. Matsuda, H. Aburatani, et al. 2004. Skeletal muscle FOXO1 (FKHR) transgenic mice have less skeletal muscle mass, down-regulated Type I (slow twitch/red muscle) fiber genes, and impaired glycemic control. *J. Biol. Chem.* 279:41114–41123. http://dx.doi.org/10.1074/jbc.M400674200

Konsman, J.P., V. Tridon, and R. Dantzer. 2000. Diffusion and action of intracerebroventricularly injected interleukin-1 in the CNS. *Neuroscience*. 101:957–967. http://dx.doi.org/10.1016/S0306-4522(00)00403-6

Kovács, K.J., A. Földes, and P.E. Sawchenko. 2000. Glucocorticoid negative feedback selectively targets vasopressin transcription in parvocellular neurosecretory neurons. *J. Neurosci.* 20:3843–3852.

Layé, S., G. Gheusi, S. Cremona, C. Combe, K. Kelley, R. Dantzer, and P. Parnet. 2000. Endogenous brain IL-1 mediates LPS-induced anorexia and hypothalamic cytokine expression. *Am. J. Physiol. Regul. Integr. Comp. Physiol.* 279:R93–R98.

Lecker, S.H., R.T. Jagoe, A. Gilbert, M. Gomes, V. Baracos, J. Bailey, S.R. Price, W.E. Mitch, and A.L. Goldberg. 2004. Multiple types of skeletal muscle atrophy involve a common program of changes in gene expression. *FASEB J.* 18:39–51. http://dx.doi.org/10.1096/fj.03-0610com

Li, W., J.S. Moylan, M.A. Chambers, J. Smith, and M.B. Reid. 2009. Interleukin-1 stimulates catabolism in C2C12 myotubes. *Am. J. Physiol. Cell Physiol.* 297:C706–C714. http://dx.doi.org/10.1152/ajpcell.00626.2008

Li, Y.-P., Y. Chen, J. John, J. Moylan, B. Jin, D.L. Mann, and M.B. Reid. 2005. TNF-alpha acts via p38 MAPK to stimulate expression of the ubiquitin ligase atrogin1/MAFbx in skeletal muscle. *FASEB J.* 19:362–370. http://dx.doi.org/10.1096/fj.04-2364com

Llovera, M., C. García-Martínez, P. Costelli, N. Agell, N. Carbó, F.J. López-Soriano, and J.M. Argilés. 1996. Muscle hypercatabolism during cancer cachexia is not reversed by the glucocorticoid receptor antagonist RU38486. *Cancer Lett.* 99:7–14. http://dx.doi.org/10.1016/0304-3835(95)04026-9

Llovera, M., C. García-Martínez, J. López-Soriano, N. Carbó, N. Agell, F.J. López-Soriano, and J.M. Argiles. 1998. Role of TNF receptor 1 in protein turnover during cancer cachexia using gene knockout mice. *Mol. Cell. Endocrinol.* 142:183–189. http://dx.doi.org/10.1016/S0303-7207(98)00105-1

Lloyd, C.E., M. Palopoli, and T.C. Vary. 2003. Effect of central administration of interleukin-1 receptor antagonist on protein synthesis in skeletal muscle, kidney, and liver during sepsis. *Metabolism*. 52:1218–1225. http://dx.doi.org/10.1016/S0026-0495(03)00161-6

Marks, D.L., N. Ling, and R.D. Cone. 2001. Role of the central melanocortin system in cachexia. *Cancer Res.* 61:1432–1438.

Minokoshi, Y., Y.-B. Kim, O.D. Peroni, L.G.D. Fryer, C. Müller, D. Carling, and B.B. Kahn. 2002. Leptin stimulates fatty-acid oxidation by activating AMP-activated protein kinase. *Nature*. 415:339–343. http://dx.doi.org/10.1038/415339a

Mitch, W.E., R. Medina, S. Grieber, R.C. May, B.K. England, S.R. Price, J.L. Bailey, and A.L. Goldberg. 1994. Metabolic acidosis stimulates muscle protein degradation by activating the adenosine triphosphate-dependent pathway involving ubiquitin and proteasomes. *J. Clin. Invest.* 93:2127–2133. http://dx.doi.org/10.1172/JCI117208

Morley, J.E., D.R. Thomas, and M.M. Wilson. 2006. Cachexia: pathophysiology and clinical relevance. *Am. J. Clin. Nutr.* 83:735–743.

Mourkioti, F., P. Kratsios, T. Luedde, Y.-H. Song, P. Delafontaine, R. Adami, V. Parente, R. Bottinelli, M. Pasparakis, and N. Rosenthal. 2006. Targeted ablation of IKK2 improves skeletal muscle strength, maintains mass, and promotes regeneration. *J. Clin. Invest.* 116:2945–2954. http://dx.doi.org/10.1172/JCI28721

Nogueiras, R., P. Wiedmer, D. Perez-Tilve, C. Veyrat-Durebex, J.M. Keogh, G.M. Sutton, P.T. Pfluger, T.R. Castaneda, S. Neschen, S.M. Hofmann, et al. 2007. The central melanocortin system directly controls peripheral lipid metabolism. *J. Clin. Invest.* 117:3475–3488. http://dx.doi.org/10.1172/JCI31743

Ogimoto, K., M.K. Harris Jr., and B.E. Wisse. 2006. MyD88 is a key mediator of anorexia, but not weight loss, induced by lipopolysaccharide and interleukin-1 beta. *Endocrinology*. 147:4445–4453. http://dx.doi.org/10.1210/en.2006-0465

Paul, P.K., S.K. Gupta, S. Bhatnagar, S.K. Panguluri, B.G. Darnay, Y. Choi, and A. Kumar. 2010. Targeted ablation of TRAF6 inhibits skeletal muscle wasting in mice. *J. Cell Biol.* 191:1395–1411. http://dx.doi.org/10.1083/jcb.201006098

Perez-Tilve, D., S.M. Hofmann, J. Basford, R. Nogueiras, P.T. Pfluger, J.T. Patterson, E. Grant, H.E. Wilson-Perez, N.A. Granholm, M. Arnold, et al. 2010. Melanocortin signaling in the CNS directly regulates circulating cholesterol. *Nat. Neurosci.* 13:877–882. http://dx.doi.org/10.1038/nn.2569

Plata-Salamán, C.R., G. Sonti, J.P. Borkoski, and C.D. Wilson; J.M. French-Mullen. 1996. Anorexia induced by chronic central administration of cytokines at estimated pathophysiological concentrations. *Physiol. Behav.* 60:867–875.

Plata-Salamán, C.R., S.E. Ilyin, and D. Gayle. 1998. Brain cytokine mRNAs in anorectic rats bearing prostate adenocarcinoma tumor cells. *Am. J. Physiol.* 275:R566–R573.

Price, S.R., J.L. Bailey, X. Wang, C. Jurkovitz, B.K. England, X. Ding, L.S. Phillips, and W.E. Mitch. 1996. Muscle wasting in insulinopenic rats results from activation of the ATP-dependent, ubiquitin-proteasome proteolytic pathway by a mechanism including gene transcription. *J. Clin. Invest.* 98:1703–1708. http://dx.doi.org/10.1172/JCI118968

Pruett, S.B., and E.L. Padgett. 2004. Thymus-derived glucocorticoids are insufficient for normal thymus homeostasis in the adult mouse. *BMC Immunol.* 5:24. http://dx.doi.org/10.1186/1471-2172-5-24

Rivadeneira, D.E., H.A. Naama, M.D. McCarter, J. Fujita, D. Evoy, P. Mackrell, and J.M. Daly. 1999. Glucocorticoid blockade does not abrogate tumor-induced cachexia. *Nutr. Cancer*. 35:202–206. http://dx.doi.org/10.1207/S15327914NC352_16

Rommel, C., S.C. Bodine, B.A. Clarke, R. Rossman, L. Nunez, T.N. Stitt, G.D. Yancopoulos, and D.J. Glass. 2001. Mediation of IGF-1-induced skeletal myotube hypertrophy by PI(3)K/Akt/mTOR and PI(3)K/Akt/GSK3 pathways. *Nat. Cell Biol.* 3:1009–1013. http://dx.doi.org/10.1038/ncb1101-1009

Ropelle, E.R., J.R. Pauli, K.G. Zecchin, M. Ueno, C.T. de Souza, J. Morari, M.C. Faria, L.A. Velloso, M.J.A. Saad, and J.B.C. Carvalheira. 2007. A central role for neuronal adenosine 5′-monophosphate-activated protein kinase in cancer-induced anorexia. *Endocrinology*. 148:5220–5229. http://dx.doi.org/10.1210/en.2007-0381

Sacheck, J.M., J.-P.K. Hyatt, A. Raffaello, R.T. Jagoe, R.R. Roy, V.R. Edgerton, S.H. Lecker, and A.L. Goldberg. 2007. Rapid disuse and denervation atrophy involve transcriptional changes similar to those of muscle wasting during systemic diseases. *FASEB J.* 21:140–155. http://dx.doi.org/10.1096/fj.06-6604com

Sandri, M., C. Sandri, A. Gilbert, C. Skurk, E. Calabria, A. Picard, K. Walsh, S. Schiaffino, S.H. Lecker, and A.L. Goldberg. 2004. Foxo transcription factors induce the atrophy-related ubiquitin ligase atrogin-1 and cause skeletal muscle atrophy. *Cell*. 117:399–412. http://dx.doi.org/10.1016/S0092-8674(04)00400-3

Scarlett, J.M., E.E. Jobst, P.J. Enriori, D.D. Bowe, A.K. Batra, W.F. Grant, M.A. Cowley, and D.L. Marks. 2007. Regulation of central melanocortin signaling by interleukin-1 beta. *Endocrinology*. 148:4217–4225. http://dx.doi.org/10.1210/en.2007-0017

Scarlett, J.M., X. Zhu, P.J. Enriori, D.D. Bowe, A.K. Batra, P.R. Levasseur, W.F. Grant, M.M. Meguid, M.A. Cowley, and D.L. Marks. 2008. Regulation of agouti-related protein messenger ribonucleic acid transcription and peptide secretion by acute and chronic inflammation. *Endocrinology*. 149:4837–4845. http://dx.doi.org/10.1210/en.2007-1680

Scheinman, R.I., P.C. Cogswell, A.K. Lofquist, and A.S. Baldwin Jr. 1995. Role of transcriptional activation of I kappa B alpha in mediation of

immunosuppression by glucocorticoids. *Science*. 270:283–286. http://dx.doi.org/10.1126/science.270.5234.283

Serrats, J., J.C. Schiltz, B. García-Bueno, N. van Rooijen, T.M. Reyes, and P.E. Sawchenko. 2010. Dual roles for perivascular macrophages in immune-to-brain signaling. *Neuron*. 65:94–106. http://dx.doi.org/10.1016/j.neuron.2009.11.032

Shimizu, N., N. Yoshikawa, N. Ito, T. Maruyama, Y. Suzuki, S.-i. Takeda, J. Nakae, Y. Tagata, S. Nishitani, K. Takehana, et al. 2011. Crosstalk between glucocorticoid receptor and nutritional sensor mTOR in skeletal muscle. *Cell Metab*. 13:170–182. http://dx.doi.org/10.1016/j.cmet.2011.01.001

Shiuchi, T., M.S. Haque, S. Okamoto, T. Inoue, H. Kageyama, S. Lee, C. Toda, A. Suzuki, E.S. Bachman, Y.-B. Kim, et al. 2009. Hypothalamic orexin stimulates feeding-associated glucose utilization in skeletal muscle via sympathetic nervous system. *Cell Metab*. 10:466–480. http://dx.doi.org/10.1016/j.cmet.2009.09.013

Stitt, T.N., D. Drujan, B.A. Clarke, F. Panaro, Y. Timofeyva, W.O. Kline, M. Gonzalez, G.D. Yancopoulos, and D.J. Glass. 2004. The IGF-1/PI3K/Akt pathway prevents expression of muscle atrophy-induced ubiquitin ligases by inhibiting FOXO transcription factors. *Mol. Cell*. 14:395–403. http://dx.doi.org/10.1016/S1097-2765(04)00211-4

Strassmann, G., M. Fong, J.S. Kenney, and C.O. Jacob. 1992. Evidence for the involvement of interleukin 6 in experimental cancer cachexia. *J. Clin. Invest*. 89:1681–1684. http://dx.doi.org/10.1172/JCI115767

Tanaka, Y., H. Eda, T. Tanaka, T. Udagawa, T. Ishikawa, I. Horii, H. Ishitsuka, T. Kataoka, and T. Taguchi. 1990. Experimental cancer cachexia induced by transplantable colon 26 adenocarcinoma in mice. *Cancer Res*. 50:2290–2295.

Tessitore, L., P. Costelli, and F.M. Baccino. 1994. Pharmacological interference with tissue hypercatabolism in tumour-bearing rats. *Biochem. J*. 299:71–78.

Tiao, G., J. Fagan, V. Roegner, M. Lieberman, J.J. Wang, J.E. Fischer, and P.O. Hasselgren. 1996. Energy-ubiquitin-dependent muscle proteolysis during sepsis in rats is regulated by glucocorticoids. *J. Clin. Invest*. 97:339–348. http://dx.doi.org/10.1172/JCI118421

Tisdale, M.J. 2009. Mechanisms of cancer cachexia. *Physiol. Rev*. 89:381–410. http://dx.doi.org/10.1152/physrev.00016.2008

Waddell, D.S., L.M. Baehr, J. van den Brandt, S.A. Johnsen, H.M. Reichardt, J.D. Furlow, and S.C. Bodine. 2008. The glucocorticoid receptor and FOXO1 synergistically activate the skeletal muscle atrophy-associated MuRF1 gene. *Am. J. Physiol. Endocrinol. Metab*. 295:E785–E797. http://dx.doi.org/10.1152/ajpendo.00646.2007

Wang, H., N. Kubica, L.W. Ellisen, L.S. Jefferson, and S.R. Kimball. 2006. Dexamethasone represses signaling through the mammalian target of rapamycin in muscle cells by enhancing expression of REDD1. *J. Biol. Chem*. 281:39128–39134. http://dx.doi.org/10.1074/jbc.M610023200

Whitaker, K.W., and T.M. Reyes. 2008. Central blockade of melanocortin receptors attenuates the metabolic and locomotor responses to peripheral interleukin-1beta administration. *Neuropharmacology*. 54:509–520. http://dx.doi.org/10.1016/j.neuropharm.2007.10.014

Wing, S.S., and A.L. Goldberg. 1993. Glucocorticoids activate the ATP-ubiquitin-dependent proteolytic system in skeletal muscle during fasting. *Am. J. Physiol*. 264:E668–E676.

Wisse, B.E., R.S. Frayo, M.W. Schwartz, and D.E. Cummings. 2001. Reversal of cancer anorexia by blockade of central melanocortin receptors in rats. *Endocrinology*. 142:3292–3301. http://dx.doi.org/10.1210/en.142.8.3292

Wu, Y., W. Zhao, J. Zhao, Y. Zhang, W. Qin, J. Pan, W.A. Bauman, R.D. Blitzer, and C. Cardozo. 2010. REDD1 is a major target of testosterone action in preventing dexamethasone-induced muscle loss. *Endocrinology*. 151:1050–1059. http://dx.doi.org/10.1210/en.2009-0530

Zamir, O., W. O'Brien, R. Thompson, D.C. Bloedow, J.E. Fischer, and P.O. Hasselgren. 1994. Reduced muscle protein breakdown in septic rats following treatment with interleukin-1 receptor antagonist. *Int. J. Biochem*. 26:943–950. http://dx.doi.org/10.1016/0020-711X(94)90088-4

Zhang, L., V. Rajan, E. Lin, Z. Hu, H.Q. Han, X. Zhou, Y. Song, H. Min, X. Wang, J. Du, and W.E. Mitch. 2011. Pharmacological inhibition of myostatin suppresses systemic inflammation and muscle atrophy in mice with chronic kidney disease. *FASEB J*. 25:1653–1663. http://dx.doi.org/10.1096/fj.10-176917

Zhou, X., J.L. Wang, J. Lu, Y. Song, K.S. Kwak, Q. Jiao, R. Rosenfeld, Q. Chen, T. Boone, W.S. Simonet, et al. 2010. Reversal of cancer cachexia and muscle wasting by ActRIIB antagonism leads to prolonged survival. *Cell*. 142:531–543. http://dx.doi.org/10.1016/j.cell.2010.07.011